mathematics

MDPI

Article

High Impedance Fault Detection Protection Scheme for Power Distribution Systems

Katleho Moloi * and Innocent Davidson *

Department of Electrical Power Engineering, Durban University of Technology, Durban 4000, South Africa
* Correspondence: katlehom@dut.ac.za (K.M.); innocentd@dut.ac.za (I.D.)

Abstract: Protection schemes are used in safe-guarding and ensuring the reliability of an electrical power network. Developing an effective protection scheme for high impedance fault (HIF) detection remains a challenge in research for protection engineers. The development of an HIF detection scheme has been a subject of interest for many decades and several methods have been proposed to find an optimal solution. The conventional current-based methods have technical limitations to effectively detect and minimize the impact of HIF. This paper presents a protection scheme based on signal processing and machine learning techniques to detect HIF. The scheme employs the discrete wavelet transform (DWT) for signal decomposition and feature extraction and uses the support vector machine (SVM) classifier to effectively detect the HIF. In addition, the decision tree (DT) classifier is implemented to validate the proposed scheme. A practical experiment was conducted to verify the efficiency of the method. The classification results obtained from the scheme indicated an accuracy level of 97.6% and 87% for the simulation and experimental setups. Furthermore, we tested the neural network (NN) and decision tree (DT) classifiers to further validate the proposed method.

Keywords: classification; high impedance fault; power system; support vector machine; wavelet packet transform

MSC: 49M41

Citation: Moloi, K.; Davidson, I. High Impedance Fault Detection Protection Scheme for Power Distribution Systems. *Mathematics* **2022**, *10*, 4298. https://doi.org/10.3390/math10224298

Academic Editors: Udochukwu B. Akuru, Ogbonnaya I. Okoro and Yacine Amara

Received: 19 September 2022
Accepted: 15 November 2022
Published: 16 November 2022

Publisher's Note: MDPI stays neutral with regard to jurisdictional claims in published maps and institutional affiliations.

1. Introduction

The power system distribution network forms an integral part of the electricity network value chain. The distribution network serves as an interlink between the power grid and the customer load segment connected into the network. Power distribution systems are prone faults. The faults occurring on the system have both technical and economic impacts. Thus, is it important to design a protection scheme that will respond efficiently to mitigate the impact of faults [1]. Over the years, overcurrent protection schemes have been successfully used to detect low impedance faults (LIF) [2]. LIFs occur when there is an insulation breakdown between the conductor phases or the conductor phases and the ground. When an LIF occurs, the fault current increases drastically, thus enabling the protection relay to detect the abnormality on the system and subsequently, tripping the circuit breaker. However, this is not the case when an HIF occurs. In case of an HIF, the current magnitude drops below a nominal current threshold value which is unlikely to be detected by conventional protection schemes. Table 1 shows the typical HIF current magnitudes on different surfaces [3]; it can be observed that the current magnitude on different surfaces may affect the protection scheme to detect the HIF accurately.

HIFs usually occur from two common cases. The first case is when a high impedance object contacts an energized power line, and the second case is when an energized power line breaks and fall on the ground. In both cases, the fault current developed is usually minimal to trigger the relay for any protective action. Unlike LIFs, HIF may cause serious

damages to the environment, humans, and animals as they can cause a fire [4]. It is imperative to design a scheme that will effectively detect HIF to minimize the adverse impact of faults.

Table 1. Fault magnitude on different surfaces [3].

Surface	Current Magnitude (A)
Dry asphalt or sand	0
Dry grass	25
Wet soil	40
Wet grass	50
Reinforced concrete	75

A significant number of methods have been proposed to find an effective solution for HIF detection. These methods range from classical to heuristic approaches. Initially, current-based methods were proposed for HIF detection. In [5,6], the authors proposed an algorithm based on current magnitude detection. However, these algorithms have often failed to detect HIFs due to the minimal or no-fault current magnitude to trigger any protection operation at the point of fault. The techniques based on harmonic content for HIF detection were proposed in [7–9], where the frequency spectrum of the HIF was used to detect the variations in the third harmonic content of the current and voltage magnitude. Based on spectrum and frequency analysis, Cui [10] proposed an algorithm based on Kalman filter (KF) analysis to detect HIF in medium voltage power systems. The application of the KF was used to estimate the effect of harmonic changes on the fault current magnitude. Other methods based on KF technique were proposed to detect the high-resolution of the current magnitude during arching [11]. The application of wavelet transform (WT) for signal interpretation has been widely used to detect HIF. In [12], the WT technique was used to distinguish the signal component of HIF from other power system operations to minimize nuisance trips. A technique based on discrete wavelet transform (DWT) and frequency range was applied to analyze and detect the signature pattern emitted by HIF [13]. A technique based on DWT and evolutionary neural network (ENN) was proposed by Silva [14]. The scheme employed the DWT technique for feature extraction and ENN for HIF classification; the scheme produced high classification results. New techniques based on wavelet transform were presented in [15–17], these techniques used DWT for feature extraction and pattern recognition to detect HIF. In [18], a technique based on DWT used the residual current magnitude on medium voltage power lines to detect HIFs. In [19], a feature extraction scheme based on discreet Fourier transform (DFT) was used to select the HIF signature from a pool of signatures. The DFT output signature was fed into the extended Kalman filter scheme to detect HIF.

Nowadays, researchers are placing more emphasis on computer intelligence-based techniques to detect HIFs. In [20], a hybrid scheme based on the energy and entropy analysis of the random behavior of the fault signal to detect HIFs was proposed. Other studies conducted in [21–24] used the practical neural network (NN)-based algorithm to detect HIF. A technique based on a combination of packet wavelet transform (PWT) and support vector machine (SVM) was proposed to detect the HIF [25]. In [26,27], the decision tree (DT) algorithms were proposed to detect HIF in low voltage power networks. The proposed algorithm produced good results. However, the technique was only used in a single-line radial network. In [28], a protection scheme based on unsupervised learning and convolutional autoencoder was proposed to detect HIF. The scheme was validated using the IEEE 13-bus test system and produced good results compared to the supervised learning systems. In another study [29], a hybrid method based on DWT and probabilistic neural network (PNN) was proposed to detect HIF. The technique used the DWT for feature selection and PNN for classification of HIF from other non-fault conditions. A technique based on (WT) for signal processing and feature selection combined with convolutional

neural network (CNN) classifier was proposed to detect HIF in power distribution network was proposed [30]. In [31], a protection scheme based on empirical mode decomposition (EMD) and artificial neural network (ANN) to detect HIF was proposed. The scheme utilized the harmonic content of the HIF current signal for classification. A protection scheme on the WT and back propagation neural network (BPNN) was proposed to detect HIF [32]. The method was tested using the data from the substation practical data and an 80% detection accuracy was achieved. Although the technical challenges of HIF detection and electricity safety in the power system industry has not yet been fully achieved, there has been significant contributions presented in the literature. Studies also show a promising trend of using artificial intelligence (AI) techniques to improve the accuracy level of HIF detection schemes. The application of using signal processing abilities of the wavelet transforms (WT) for feature extraction and pattern recognition has been widely used to enhance efficiency of protection technology [33,34].

Mathematical models form an integral part of designing rigorous fault diagnostic techniques in power systems engineering. Most of the engineering solutions have been developed using mathematical approaches. In the present work, we propose the application of mathematical models using machine learning techniques to solve an engineering problem. The proposed hybrid model demonstrates the applicability of mathematical models in the engineering fraternity. Our model integrates various segments of mathematics which includes signal processing, feature extraction, optimization, and pattern recognition. For instance, at the initial stage of our model, a fault signal is decomposed using DWT to analyze the segments of interest from the unabridged fault signal spectrum; thereafter, a feature extracting technique is employed using the mathematical statistical features to select specific features from the entire data spectrum, subsequently these features are used as inputs to train, test, and validate the pattern recognition and classification mathematical algorithm using SVM. Lastly, the GA technique (Table A1) uses the biological concept to optimize the parameters of the SVM classifier (Table A2) and thus improving the classification accuracy. The main contribution of the study is to exhibit the interrelation between mathematics and engineering.

2. Feature Extraction Based on Discrete Wavelet Transform

Feature extraction can be defined as a mathematical technique used to decode high dimensional data sets into a smaller dimension without losing the content of the actual data set. Thus, feature extraction is an essential segment of the protection scheme which is used to improve the fault classification [35]. In the present work, statistical features are extracted at each level of signal decomposition. The feature includes the energy and entropy of the fault signal.

2.1. Wavelet Transforms

WT has appeared as a powerful signal processing technique for signal decomposition and feature extraction over the traditional Fourier transforms [36,37]. There are two mostly used WTs, namely the continuous wavelet transforms (CWT) and DWT techniques. The CWT of a given $x(t)$ signal can be calculated as:

$$CWT(a,b) = \frac{1}{\sqrt{a}} \int_{-\infty}^{+\infty} x(t)\,\psi\left(\frac{t-b}{a}\right) dt \quad (1)$$

where, a and b represents the scaling and translation factors. Similarly, the DWT can be defined mathematically as:

$$DWT(m,n) = \frac{1}{\sqrt[m]{a}} \sum_{k} x(k)\,\psi\left(\frac{k - nb_0 a_0^m}{a_0^m}\right) dt \quad (2)$$

where, a and b in Equation (1), are transformed to be the functions of integers m, n, k. The DWT technique can be used to effectively recognize non-stationary signals. The decomposition process is performed using the multiresolution analysis technique (MRA). The process is shown in Figure 1. The process begins with a signal passing through both the high and low pass filters. The low pass filter is replicated by the approximation coefficient (c_j) and the high pass filter is replicated by the detail coefficient (d_j). At each level of decomposition, the detail coefficient information from the high pass filter is discarded before the process is re-established in the next level of decomposition. The most important aspect of using WT technique is the proper selection of a mother wavelet. The approximation and detail coefficients are mathematically represented as:

$$c_j = \sum_k x(n).h(2n-k) \tag{3}$$

$$d_j = \sum_k x(n).g(2n-k) \tag{4}$$

where, c_j is the output from the low pass filter which replicates the approximation coefficients of the original signal, and d_j is the output from the high pass filter which replicates the detail coefficient of the original signal.

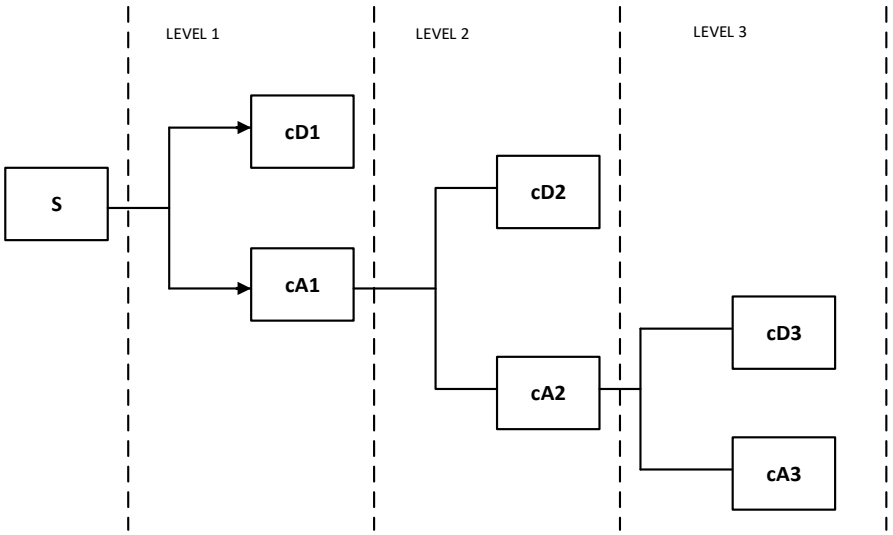

Figure 1. MRA decomposition tree.

2.2. Feature Extraction

Feature extraction techniques are valuable tools used as a foundation to most power system classification and regression problems. Feature extraction techniques are used to reduce high dimension data spectrum to a minimized sizable data spectrum without losing the essence of the original data set. In the current work, the two statistical features extracted from the reconstructed signal are the energy and the entropy of the signal. The energy of the fault current signal $y(t)$ is given by:

$$E(t_1, t_2) = \int_{t_1}^{t_2} [y(t)]^2 \, dt \tag{5}$$

where, t_1, t_2 represents the time range for the energy measurement. The entropy EN of the signal $y(t)$ such that $E(0) = 0$ is given by:

$$EN(y) = \sum_i EN(y_I) \tag{6}$$

where, y_I is the decomposed coefficient of the original signal $y(t)$, and EN is the approximated entropy. A feature matrix is formulated based on the energy and entropy measurements and subsequently used as input to the classifiers.

3. High Impedance Fault Classification Based on Support Vector Machines

Classification is a mathematical process used to identify specific features of interest from a wide range of features. This phenomenon has been widely used in power systems for condition monitoring. It is important to design protection schemes with rigorous pattern recognition abilities to enable prompt protection responses during fault conditions.

3.1. Support Vector Machines

SVMs form part of the statistical learning techniques based on structural risk minimization methods. SVMs have been successfully used in power systems for pattern recognition and classification problems [38]. The objective of using SVMs is to find a separating margin between two different classes of data called the hyperplane. The hyperplane is determined by mapping the input vectors into a high dimensional space. Generally, a hyperplane is set to be optimal under two conditions, (a) if the data classes are separated by a greater margin, and (b) if the distance between the closest data class and the hyperplane is maximal [39]. Suppose we are given the input training data $(x_1, y_1), (x_2, y_2), \cdots (x_l, y_l)\ x_i \epsilon R^n, y_i \epsilon [+1, -1]$. x_i indicates the input patterns, and y_i is the desired target output, for instance, y_i belongs to the −1 class when the data value is -0.1, and y_i belongs to the +1 class when the data value is +0.1. The input data is mapped into a feature space by means of a non-transformation function Φ.

$$\Phi: R^n \longrightarrow F^m\ x_i \longrightarrow \Phi.(x_i) \tag{7}$$

The data are subsequently separated by using the function f in the high dimensional space. The dimensional space (Y^2) where $(Y\epsilon\{+1, -1\})$ is mapped by applying the function f and is given by:

$$f: F^m \longrightarrow Y^2\ \Phi.(x_i) \longrightarrow f\big(\Phi.(x_i)\big) \tag{8}$$

Suppose the data are linearly separable, the vector dimension is given $w \epsilon R^N$ and the scaler dimension is given by $b\epsilon R$, such that the desired output $y_i(w.x_i + b) \geq 1\ \forall$ data parameters within the training set $(i = 1,2, \cdots l)$. Consequently, the hyperplane can be determined by computing $w.x + b = 1$ for the data points nearer to the plane on one side and, $w.x + b = -1$ for the data points nearer on the other side of the plane. Thus, the optimal hyperplane can be computed by solving the quadratic programming problem given by:

$$min \frac{1}{2}\|w^2\| + C\left(\sum_{I=1}^{L} \varepsilon_I\right) \tag{9}$$

Subject to $y_i(w.x_i + b) \geq 1 - \varepsilon_I,\ \varepsilon_I \geq 0\ \forall i$

The optimized problem formulation is solved by using the Langrangian multipliers defined as:

$$\lambda(w, b, a) = \frac{1}{2}\|w^2\| - \sum_{l=1}^{l} \alpha(y_i\,(w.x_i + b) - 1 \tag{10}$$

where, w, b are the primal variables, and α is the dual variable, which are used to minimize the Langrangian function. The solution vector in terms of the training design is computed by using the Karush–Kuhn–Tucker (KKT) conditions. Consequently, upon solving the optimization problem, the training points with $\alpha_i > 0$ are referred to as support vectors (SVs). The primal variables w and b can be calculated as:

$$w = \sum_{i=1}^{l} \alpha_i \, y_i x_i \tag{11}$$

$$b = y_{sv} - \sum_{i=1}^{l} \alpha_i \, y_i . k(x, x_i) \tag{12}$$

where, x represents the test vector. Suppose that $\alpha_i \neq 0$ and sgn is the signal function, the optimal decision function can be expressed mathematically as:

$$f(x) = sgn \, (\sum_{i=1}^{l} \alpha_i \, y_i . k(x, x_i) + b \tag{13}$$

where, k is the kernel function and it is computed by determining the inner product $\langle \Phi(x_i), \Phi x_j \rangle$ in the feature space as a function of the input data set. The classification of HIF and non-fault conditions is achieved by using different kernel functions, such as the linear, quadratic, and radial bias function 38.

3.2. Decision Tree

The decision (DT) algorithm has been widely used in pattern recognition and classification purposes. The main quality of the DT algorithm is its ability to maximize and fix the data division 39. When using the DT algorithm, the data set is spilt into numerous branches recursively. This process is repeated until the classification efficiency is achieved. Subsequently, the DT algorithm is mathematically defined as:

$$\bar{X} = \{X_1, X_2, \cdots X_m\}^T \tag{14}$$

$$X_i = \{x_1, x_2, \cdots, x_{ij}, \cdots, X_{in}\} \tag{15}$$

$$S = \{S_1, S_2, \cdots, S_i, \cdots, S_m\} \tag{16}$$

where, $m, n,$ and $S,$ represents the number of observations, the independent variable number and the dimensional vector of the variables forecasted from $\bar{X}$. The ith component of the is represented by X_i. The $x_1, x_2, \cdots, x_{ij}, \cdots, X_{in}$_in represents the autonomous variable of the component vector, and T is the transpose natation vector. The fundamental desired output of using the DT algorithm is to predict the $S,$, based on the $\bar{X}$ variables. The challenge of using the DT algorithm is to obtain a best possible tree for efficient classification due to high space dimension. It is for such reason that an optimal DT algorithm tree T_{k0} is designed by solving the optimization problem defined mathematically by:

$$\hat{R}(T_{k0}) = \min_k \{\hat{R}T_k\}, \; k = 1,2,3 \ldots, K \tag{17}$$

$$\hat{R}(T) = \sum_{t \in \tilde{T}} \{r(t)p(t)\} \, (16) \tag{18}$$

where, $\hat{R}(T)$ represents the misclassification error of T_k, T_{k0} is the optimal DT algorithm to curtail the classification error, T is the binary tree $\in \{T_1, T_2, T_3 \ldots, T_k, t_1\}$, k, t and t_1 represent the tree index, the tree node and the root node respectively, $r(t)$ represent the estimate of classification error in node t and $p(t)$ represents the probability of any case that may drop into node t. Generally, the implementation of the DT algorithm is simple and produces good results for classification purposes.

4. Proposed Protection Scheme for High Impedance Fault Detection

The detection of HIF with high accuracy has been a technical problem for protection engineers over the years [39]. The difficulties with HIF detection are well documented and several techniques have been proposed. In this section, the proposed method for HIF detection using DWT-GA-SVM scheme is discussed. The method uses the first cycle of the

fault current measured at the source terminal after the occurrence of the fault. Subsequently, the measured current is passed through both the high and low pass filters by means of the DWT technique. The signal is analyzed, thus obtaining the detail and approximation coefficients using the MRA technique. The decomposition process is computed until the fourth level. Subsequently, the statistical features (energy and entropy) are extracted from the detail coefficient of the reconstructed signal at level 4. The GA technique is used to optimize the parameters of the extracted features used to train and test the SVM and DT for classification of HIF and other power system operations. The logic architecture of the proposed method is given in Figure 2.

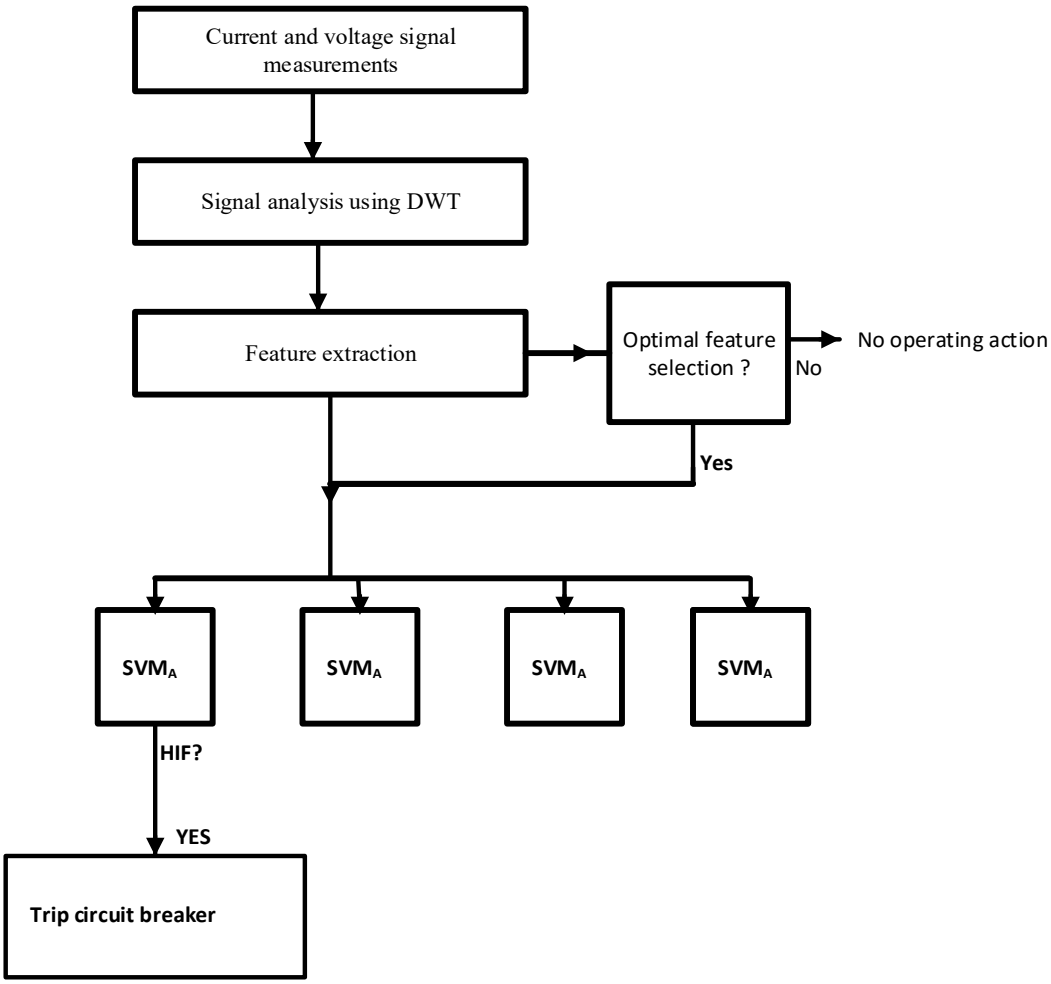

Figure 2. Wavelet transform and support vector machine fault classification scheme.

4.1. Selection of Mother Wavelet

The selection of a mother wavelet is an important aspect of utilizing DWT for signal processing. Essentially, DWT has been used effectively to decompose and extract features from non-stationary signals. In the present work, six (6) mother wavelets were tested using the statistical measures to validate the choice of selection. The comparison was acquired by computing the standard deviation, mean deviation and median absolute deviation. In Table 2, the mother wavelet selection is depicted. From the obtained analysis, the Daubechies (db4) yielded the best results compared to the other mother wavelets and thus was selected for the purposes of the current study.

Table 2. Selection of mother wavelet.

Mother Wavelet	Standard Deviation	Mean Deviation	Median Absolute Deviation
Db4	2.112	2.505	1.955
Db7	3.450	2.913	2.085
Db14	3.551	2.588	2.910
Sym4	2.941	3.528	3.201
Sym7	2.887	3.415	2.580
Sym14	3.815	3.117	3.155

4.2. SVM Implementation

SVMs have been widely used to solve both the classification and the regression problems in power systems. To minimize the computational and design complexity, four (4) SVMs are used and each SVM is trained to classify and detect HIF and other power system operating conditions. The other power system operating conditions include the capacitor switching (CS), load switching (LS) and normal operation (NO). The four (4) SVMs, are arranged chronologically as: SVM_A for HIF, SVM_B for CS, SVM_C for LS, and SVM_D for NO respectively. The output of each SVM is either +1 or -1, where +1 indicates that an operation has occurred in the corresponding SVM, and -1 means there is no operation in any of the SVMs. In Table 3, the SVM training matrix is depicted. The matrix would then be used to send a trip pulse to a circuit breaker in a case of an HIF. For instance, the output $[+1, -1, -1, -1]$ would correspond to the presence of HIF leading to a decision to operate the circuit breaker.

Table 3. SVM classification matrix.

Type of Incident	SVM_A	SVM_B	SVM_C	SVM_D
HIF	+1	−1	−1	−1
CS	−1	+1	+1	−1
LS	−1	−1	+1	−1
NO	−1	−1	−1	+1

5. Power Distribution System: Case Study

To demonstrate the validity of the proposed method, an Eskom power distribution system is studied. The model is carried out using the DIgSILENT PowerFactory engineering software tool. Eskom is South Africa's dominant electric utility responsible for over 95% of power generation and exporting to some neighbouring countries in Southern Africa. The reduced network segment consists of a substation at 132/22 kV with three outgoing 22 kV feeders named (Siyabuswa 22kV, Verena 22 kV, and Amanda 22kV). The substation parameters and distribution line parameters are shown Tables 4 and 5, respectively. Additionally, in this paper an HIF case is modelled based on an improved model proposed in [30]. The model consists of a sending node model based on an AC source supply, two impedances based on the capacitance, resistance, and inductance of the power system. The other distinctive property regarding HIF cases is the non-linearity of the current magnitude at each cycle of the signal. One major challenge with HIF detection is the similarity in nature with other power system operation signals such as capacitor switching, non-linear load switching, and inductive load switching. It is thus imperative, to develop a scheme that can distinguish HIF from other power system operations to minimize the incorrect tripping of the breaker. Consequently, in this paper, such operations are considered for the validation of the scheme. Moreover, low impedance fault such as single line, double line, and three phase faults are included to improve the validity of the scheme.

Table 4. Substation source parameters.

Substation Source	Short Circuit Power (MVA)	Short Circuit Current (kA)	X/R	X_1/X_0	R_1/R_0
Parameters	1140	15.3	132.1	0.55	0.61

Table 5. Distribution line parameters.

Feeder (22 kV)	Length (km)	Pos = Neg. Seq. $R_1 = R_2$ (Ω/km)	Pos = Neg. Seq. $X_1 = X_2$ (Ω/km)	Zero. Seq. R_0 (Ω/km)	Zero Seq. X_0 (Ω/km)
Siyabuswa	15.3	0.119	0.168	0.145	1.850
Amandla	12.8	0.119	0.168	0.145	1.850
Verena	19.6	0.119	0.167	0.145	1.850

HIF Modelling

The accurate modelling of HIF has been a challenge to many engineers over the years, although several models have been proposed. In the current study we adopted a high resistance and dynamic model to formulate HIF. We assumed that the HIFs exit because of the tree contacting the energized medium voltage line. The dynamic model is given by:

$$\frac{dg}{dt} = \frac{1}{\tau}(G - g) \tag{19}$$

$$G = \frac{|i|}{V_{arc}} \tag{20}$$

$$\tau = Ae^{Bg} \tag{21}$$

where, g, G, represents the time-varying conductance and stationary arc conductance, respectively, the arc current absolute is given by $|i|$, the time constant is given by τ, V_{arc} is the arc voltage parameters, A and B are the arc constants.

6. Results and Discussion

This section discusses the simulation results of HIF and other power system cases. The signal processing of a fault current improves the classification scheme. The DWT has been successfully used to analyze and track points of interest withing a range of a signal. However, the selection of a mother wavelet is an essential part of using DWT efficiently. As depicted in Table 2, a db4 mother wavelet was selected for purposes of signal decomposition. Some of the fourth level decomposition coefficients are depicted in Figure 3. The simulations were performed using the sampling frequency of 12.5 kHz.

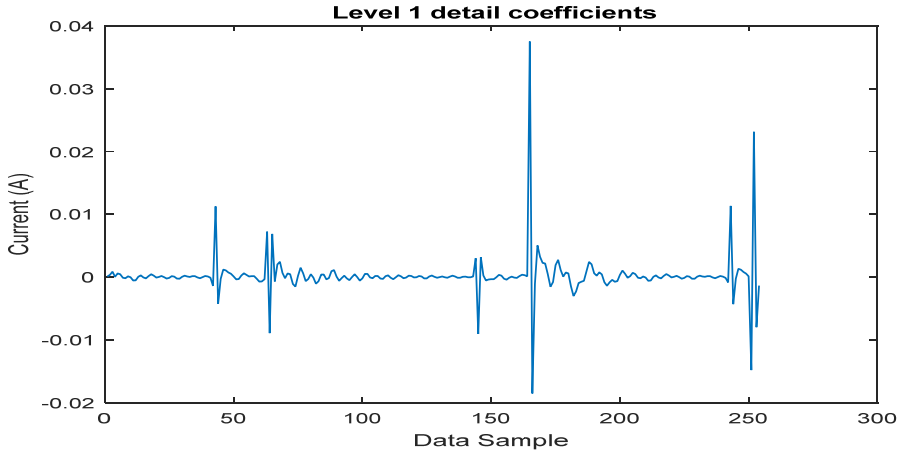
Level 1 detail coefficients
Current (A)
Data Sample
0.04
0.03
0.02
0.01
0
-0.01
-0.02
0
50
100
150
200
250
300

(**a**)

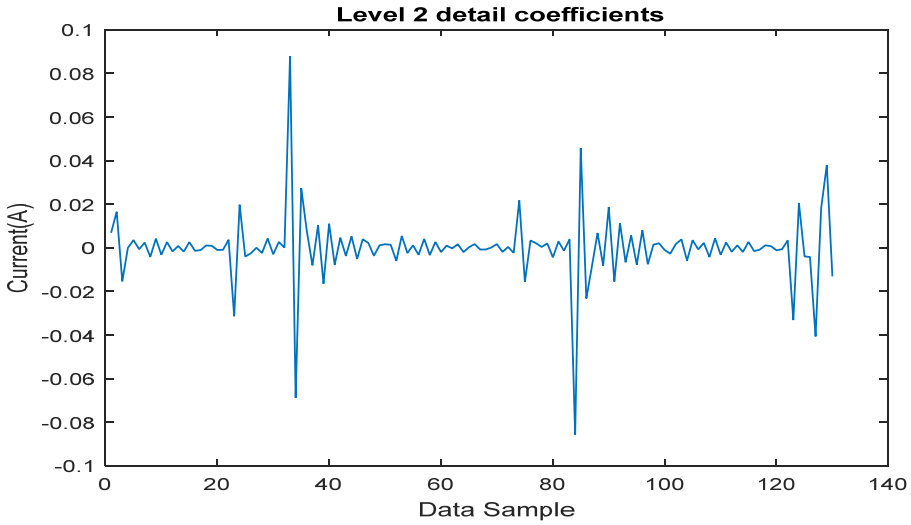
Level 2 detail coefficients
Current(A)
Data Sample
0.1
0.08
0.06
0.04
0.02
0
-0.02
-0.04
-0.06
-0.08
-0.1
0
20
40
60
80
100
120
140

(**b**)

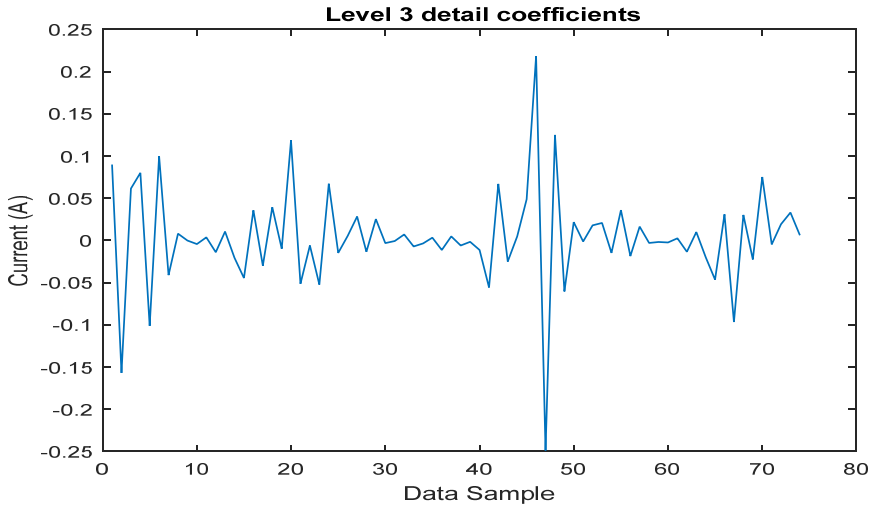
Level 3 detail coefficients
Current (A)
Data Sample
0.25
0.2
0.15
0.1
0.05
0
-0.05
-0.1
-0.15
-0.2
-0.25
0
10
20
30
40
50
60
70
80

(**c**)

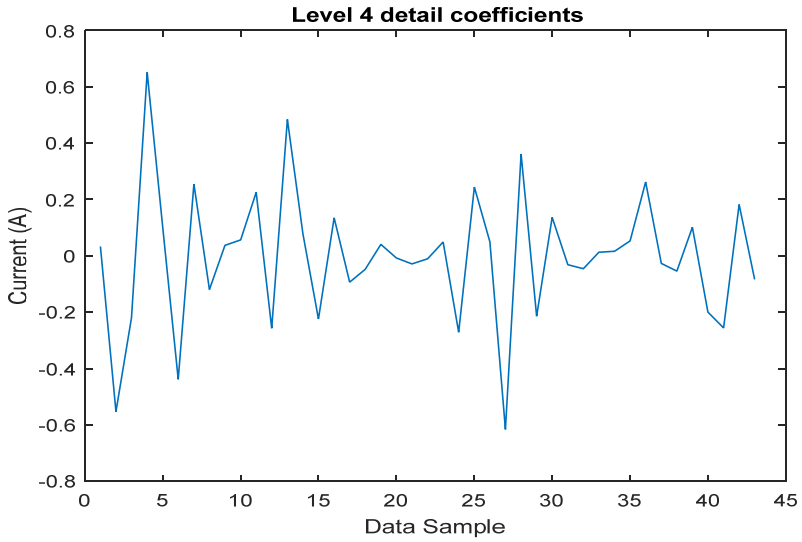

(**d**)

Figure 3. (**a**)-(**d**) level decomposition.

The HIF current signal obtained from the simulation platform is shown in Figure 4. The results emphasize the random behavior of HIF signals. As indicated by the signal, the positive and negative cycles exhibit different current magnitudes for a similar fault. In addition, the fault magnitude depletes with time resulting in difficulties of detection. Generally, HIFs are associated with arching. This phenomenon of arching has been widely used to develop the possible detection schemes for HIFs. The HIF arc voltage is shown in Figure 5. The signal indicates a significant increase on the voltage at the incipient of the fault. However, the signal is not uniformly distributed and decreases in magnitude over time.

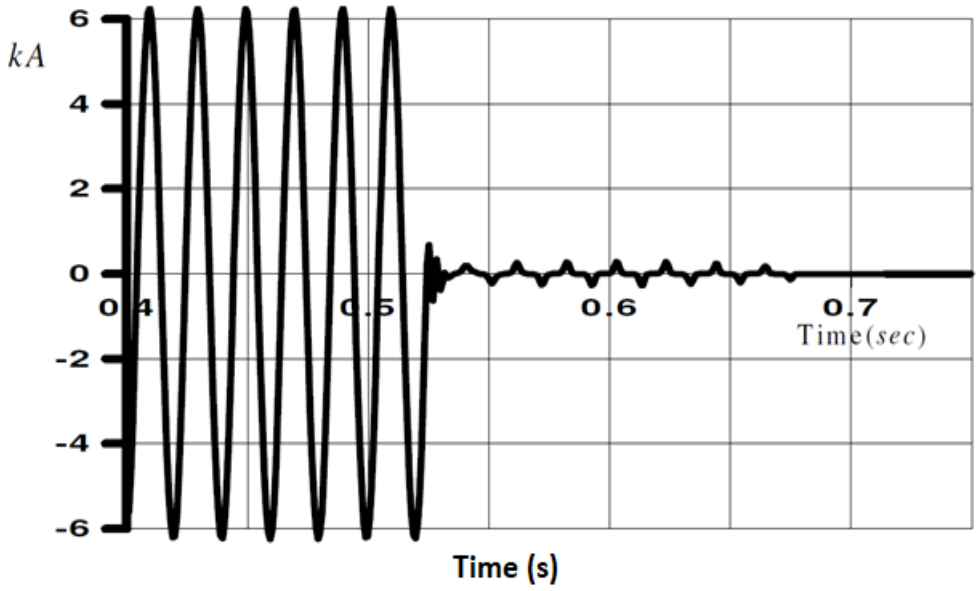

Figure 4. HIF current signal.

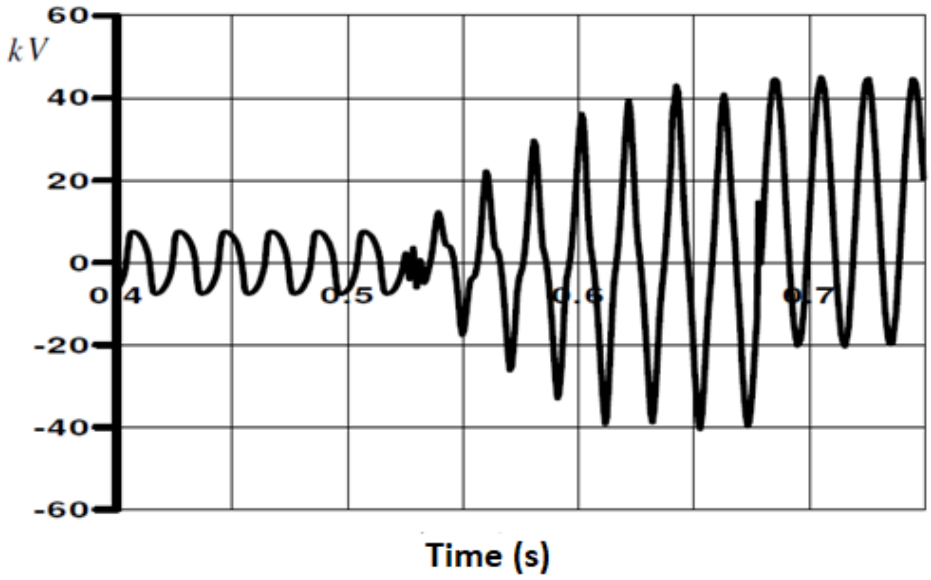

Figure 5. HIF arc voltage.

6.1. Classification of HIF

The art of protection engineering encompasses the segment of classification. In technical terms, classification can be defined as a systematic method of organizing features according to their category. In the present work, the SVM, DT, and NN mathematical techniques are used primarily to classify HIF and other technical operations on the power system. The description of the different signal events considered for the classification schemes is shown in Table 6.

Table 6. Description of different signal events.

Signal Events	Class Identification
High impedance fault	A1
Normal current	A2
Capacitor switching	A3
Inductor switching	A4
Load switching	A5
Line to ground fault	A6
Line to line fault	A7
Line to line to ground fault	A8
Three phase fault	A9
Three phase fault to ground	A10

The classification accuracy of signal events (A1-A5) and (A6-A10) using the SVM and DT techniques are shown in Tables 7 and 8, respectively. The results show 97.3% accuracy using SVM for signal events (A1–A5) and 95.5% accuracy using the DT technique, as well as an accuracy level of 98.5% and 97.8% using the SVM and DT techniques for (A1–A5) and (A6–A10), respectively. To demonstrate the effectiveness of using the GA technique for optimal feature selection, a comparison between the optimal features and non-optimal features used for classification is shown in Table 9.

Table 7. Classification of A1-A5 signal events.

SVM						**DT**				
	A1	**A2**	**A3**	**A4**	**A5**	**A1**	**A2**	**A3**	**A4**	**A5**
A1	96	1	0	0	1	95	2	0	0	1
A2	2	94	2	1	0	1	95	0	2	1
A3	2	0	95	1	2	1	0	96	2	2
A4	1	1	0	98	1	1	1	0	97	0
A5	0	2	1	2	96	0	1	2	1	98
Accuracy (%) = 97.3						Accuracy (%) = 95.5				

Table 8. Classification of A6-A10 signal events.

SVM						**DT**				
	A6	**A7**	**A8**	**A9**	**A10**	**A6**	**A7**	**A8**	**A9**	**A10**
A6	98	1	0	0	1	97	1	2	0	1
A7	1	93	1	1	0	1	98	0	1	0
A8	1	0	97	1	1	0	1	98	0	0
A9	1	1	0	92	1	0	0	2	95	1
A10	0	1	1	0	98	1	2	1	0	95
Accuracy (%) = 98.5						Accuracy (%) = 97.8				

The performance of the SVM, DT and NN classifiers is presented Tables 9–11 respectively. The results show that SVM has a high accuracy level compared to the DT and NN classifiers. The accuracy precision of the SVM, DT, and NN is given by 97.6%, 96.5%, and 95.4%, respectively.

Table 9. SVM classification performance.

Class	**TP**	**FP**	**Precision**	**Recall**	**F-Measure**	**ROC**
A1	0.952	0.000	0.975	0.966	0.983	0.988
A2	0.919	0.000	1.000	0.965	0.960	0.967
A3	0.966	0.000	0.952	0.958	0.983	0.988
A4	0.935	0.002	0.955	0.938	0.966	0.985
A5	0.953	0.001	0.985	0.933	0.980	0.976
A6	0.950	0.000	1.000	0.960	0.966	0.958
A7	0.961	0.004	0.998	0.955	0.952	0.960
A8	0.911	0.001	0.952	0.961	0.955	0.976
A9	0.915	0.004	0.965	0.979	0.982	0.971
A10	0.973	0.043	0.980	0.982	0.904	0.988
Avg	0.944	0.006	0.976	0.961	0.961	0.976

Table 10. DT classification performance.

Class	**TP**	**FP**	**Precision**	**Recall**	**F-Measure**	**ROC**
A1	0.991	0.000	0.960	1.000	0.991	0.970
A2	0.920	0.000	0.991	0.990	0.990	0.966
A3	0.933	0.000	0.990	0.980	0.995	0.985
A4	0.985	0.000	0.961	0.985	0.977	0.990
A5	0.968	0.003	0.950	0.930	0.988	0.900
A6	0.987	0.000	0.910	0.975	0.970	0.988
A7	0.980	0.014	0.960	0.957	0.966	0.955
A8	0.981	0.010	0.988	0.911	0.960	0.975
A9	0.971	0.035	0.991	0.980	0.991	0.961

A10	0.981	0.043	0.950	0.990	0.955	0.992
Avg	0.969	0.011	0.965	0.970	0.978	0.968

Table 11. NN classification performance.

Class	TP	FP	Precision	Recall	F-Measure	ROC
A1	0.902	0.000	0.915	0.990	0.905	0.955
A2	0.915	0.000	0.943	0.955	0.922	0.950
A3	0.945	0.000	0.955	0.965	0.959	0.980
A4	0.955	0.000	0.940	0.952	0.960	0.970
A5	0.915	0.003	0.933	0.911	0.977	0.911
A6	0.920	0.010	0.990	0.933	0.950	0.916
A7	0.991	0.000	0.982	0.960	0.960	0.958
A8	0.900	0.010	0.922	0.915	0.955	0.988
A9	0.980	0.050	0.985	0.930	0.965	0.966
A10	0.975	0.045	0.975	0.945	0.977	0.911
Avg	0.941	0.012	0.954	0.946	0.953	0.951

The screenshots demonstrating the impact of the kernel function to maximize the hyperplane and thus, improving classification accuracy between HIF and LS, and HIF and CS are depicted in Figures 6 and 7, respectively. As shown in both figures, the hyperplane maximally separates the two different classes of data events and thus improving the accuracy of the protection scheme.

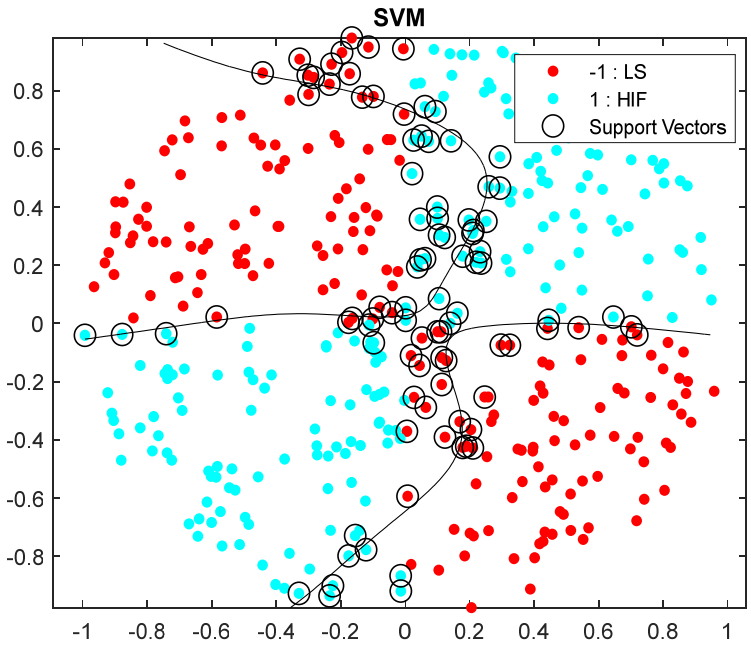

Figure 6. SVM classification between HIF and LS.

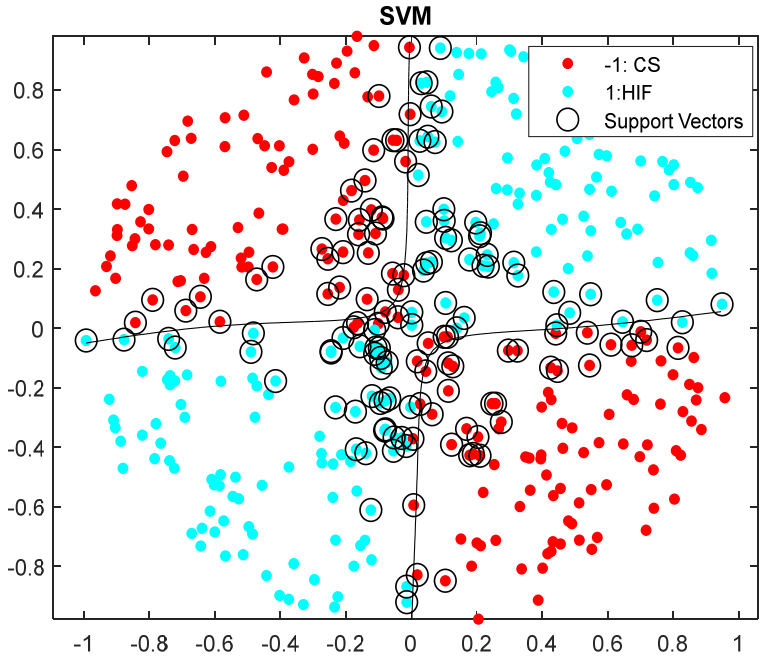

Figure 7. SVM classification between HIF and CS.

6.2. Experimental Analysis

To validate the proposed HIF detection scheme, an experimental setup was conducted. The experiment was conducted at a high voltage engineering lab in Mpumalanga province in South Africa. The experimental data are presented in Table 12.

Table 12. Experimental setup data.

Description	Parameters
Source	5 A, 50 Hz, 2.5% short circuit impedance using transformer
Transformer	10 kVA, 110/132 kV, 4.5%
Capacitor	High Voltage 100 pF, 100 kV, Low voltage 100 nF
Atmospheric conditions	T = 31 °C

The electrical circuit and experimental setup for HIF detection is shown in Figures 8 and 9, respectively. The instrument used to perform the experiment is the ICM8 power analyzer. The HIF voltage and current magnitude measured from the experimental setup are shown in Figure 10 and Figure 11, respectively. To accurately measure the experimental parameters, the experimental error of margin must be minimized. These errors occur as a result of the measuring instruments such the voltage transformer, the current transformer, and the ICM8 power analyzer. Another element which may increase the error is the saturation of both the voltage and current transformers. However, in the case of HIF the current magnitude is minimum and such fault cannot lead to saturation. Thus, during the HIF, the current transformer operates linearly.

The experiment was conducted in two stages. In the first stage, the tree resistance was measured when there was physical contact between the tree and the energized conductor. The voltage applied on the tree was then increased steadily in steps to measure the current and the voltage values and thus, estimated the tree impedance as shown in Figure 12. The dotted line was obtained using the experimental data and the solid line gives the initial resistance value. The resistance value also depends on the atmospheric conditions and the location on the tree where the measurement is obtained. In the second stage of the experiment, the voltage was applied to the conductor while moving the tree

very close to the energized conductor resulting in an arc. The movement of the tree from the energized conductor varied between 2-5 cm; in these instances, the arc current was established.

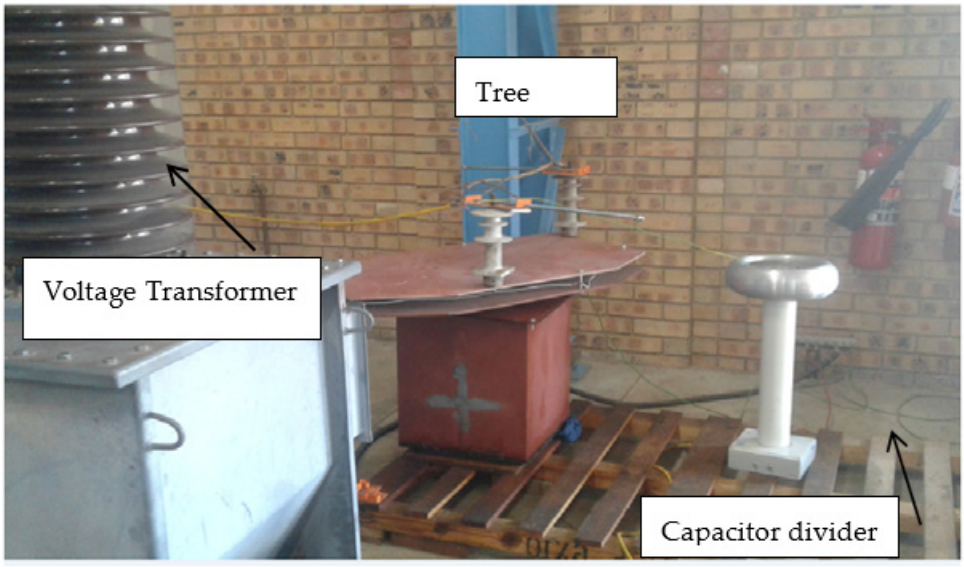

Figure 8. HIF experimental setup.

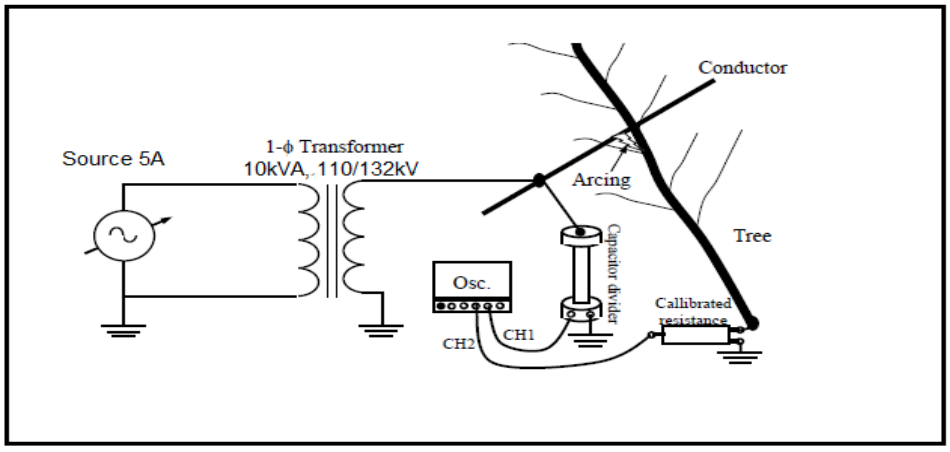

Figure 9. HIF electrical circuit.

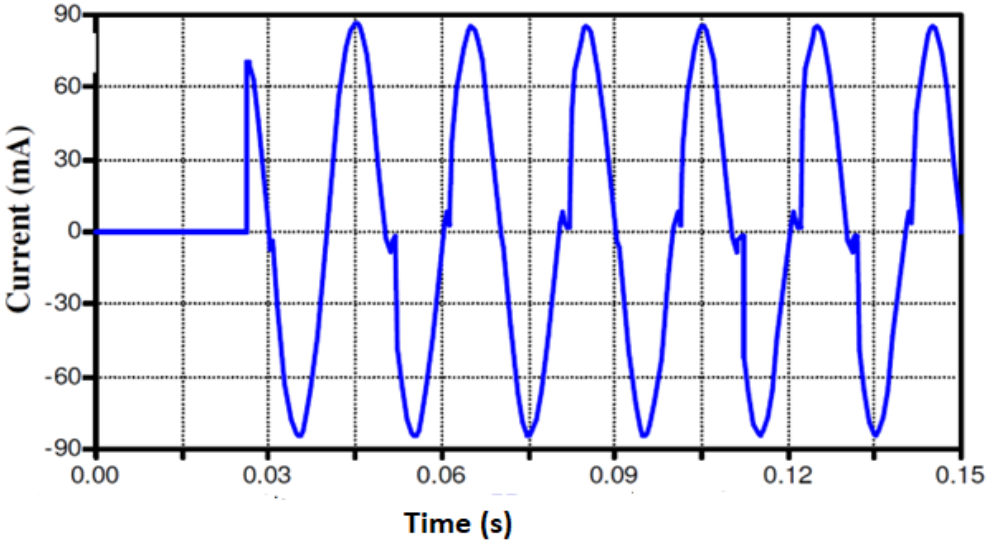

Figure 10. HIF current and voltage measurements.

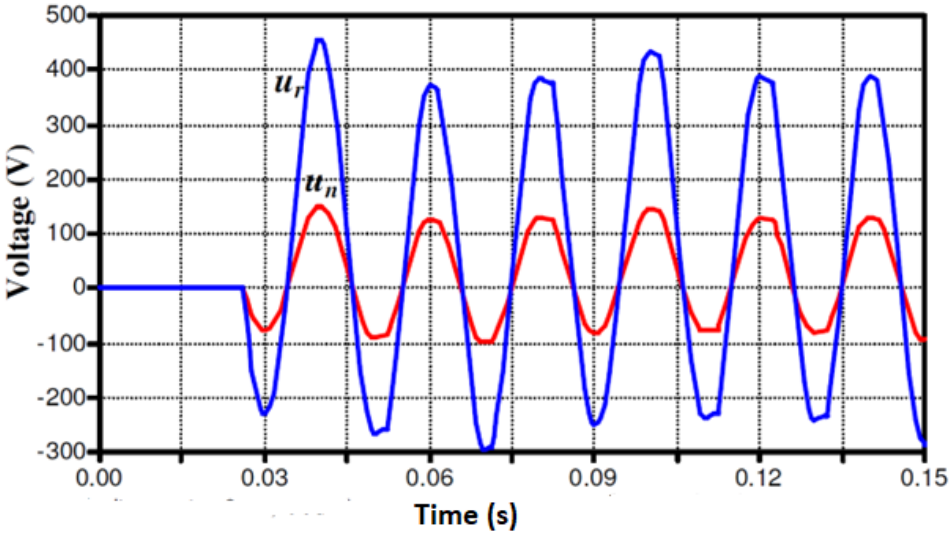

Figure 11. Measure neutral (U_n), and residual voltage (U_r).

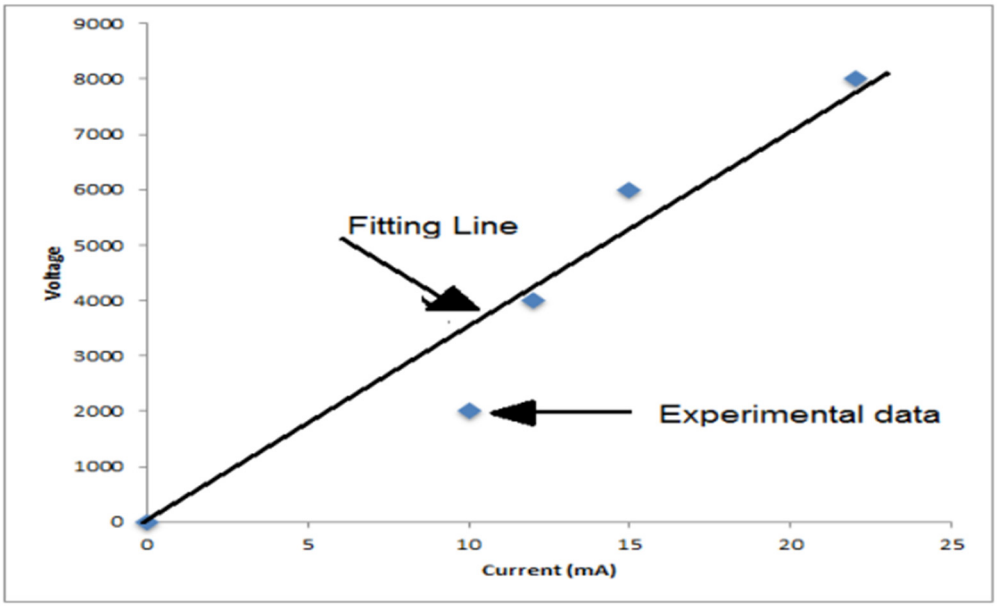

Figure 12. Tree resistance measurement.

The results of the classification validation of the proposed scheme for the simulation and experimental based analysis are presented in Tables 13 and 14, respectively. From the results presented in Table 13, the classification accuracy of SVM is reported to be 97.6% compared to the DT and NN classification results of 96.5% and 95.4%, respectively. In addition, the time required to classify the fault using SVM is reported to be 0.90ms compared to the time required to classify the fault by the DT and NN classifiers. These results emphasize the importance of computational efficiency and processing time reduction. Thus, our proposed model uses less time to detect the fault with high accuracy. The classification accuracy is determined by calculating the ratio between the correctly classified instances and the total instance tested.

Table 13. Classification accuracy of different classifiers using simulation data with GA.

Classifiers and Wavelet	Time Required to Build Model (Minutes)	Time Required to Classify the Fault (ms)	Total Number of Instances	Total Number of Correctly Classified Instances	Total Number of Incorrectly Classified Instances	Accuracy (%)
SVM & DWT	2.51	0.90	4000	3904	96	97.6
DT & DWT	10.3	0.92	4000	3860	140	96.5
NN & DWT	15.3	0.95	4000	3816	184	95.4

Table 14. Classification accuracy of different classifiers using experimental data with GA.

Classifiers	Time Required to Build Model (Minutes)	Time Required to Classify the Fault (ms)	Total Number of Instances	Total Number of Correctly Classified Instances	Total Number of Incorrectly Classified Instances	Accuracy (%)
SVM	1.25	0.75	100	87	13	87.0
DT	3.22	0.88	100	85	15	85.0
NN	4.50	0.91	100	83	17	83.0

7. Conclusions

In this study, we proposed an HIF detection technique. The technique uses mathematical models for signal analysis, feature extraction, optimization, and classification to

detect the HIF. The study of HIF has been conducted over many years to find an optimal solution. Generally, HIF can cause severe consequences such as infrastructure damage and possible human fatalities. It therefore is imperative to design a protection scheme that will effectively detect HIF. In the present work, a hybrid mathematical protection scheme is proposed; the scheme uses DWT to decompose and analyze different fault signals using the db4 mother wavelet. Thereafter, the statistical features from the decomposed signals are extracted to build a feature matrix. Consequently, the feature matrix is used to test, train, and validate the SVM classifier. The GA is used to improve the performance of the classifier. The results presented depict that HIF can be detected with an accuracy level of 97.6% using SVM compared to the DT and NN classifier with accuracy levels of 96.5% and 95.4%, respectively, for simulation-based data instances. Finally, we conducted an experiment to test the validity of the proposed method. The experimental results show that the HIF can be classified correctly using SVM with an accuracy of 84% compared to the classification accuracy 85% and 83% when using the DT and NN classifiers, respectively. The development of a hybrid protection for HIF detection is made possible by using mathematical models. In future studies, the HIF detection with high penetration levels of renewable distributed generation will be considered.

Author Contributions: Conceptualization, K. M., and I. D.; methodology, K.M.; software, K.M.; validation, K. M and I. D.; formal analysis, K.M.; investigation, K.M.; resources, I.D., data curation, K.M.; writing—original draft preparation, K.M.; writing—review and editing, I.D.; visualization, I.D.; supervision, I.D.; project administration, K.M.; funding acquisition, I.D. All authors have read and agreed to the published version of the manuscript.

Funding: This research received no external funding.

Institutional Review Board Statement: Not applicable**.**

Informed Consent Statement: Not applicable.

Data Availability Statement: Not applicable.

Conflicts of Interest: The authors declare no conflict of interest.

Appendix A

In this section, the GA, and SVM parameters are given in Tables A1 and A2, respectively.

Table A1. GA parameters.

Parameter	Value
Probability of mutation (pm)	0.005
Probability of cross over (pc)	0.010
Population size (N)	1000

Table A2. SVM parameters.

SVM	RBF Kernel Parameters
SVM_A	$\gamma = 50$ σ^2
SVM_B	$\gamma = 50$ σ^2
SVM_C	$\gamma = 50$ σ^2
SVM_D	$\gamma = 50$ σ^2

References

1. Moloi, K.; Yusuff, A.A. A Support Vector Machine Based Fault Diagnostic Technique in Power Distribution Networks. In Proceedings of the 2019 Southern African Universities Power Engineering Conference/Robotics and Mechatronics/Pattern Recognition Association of South Africa (SAUPEC/RobMech/PRASA), Cape Town, South Africa, 28–30 January 2019.
2. Magagula, X.G.; Hamam, Y.; Jordaan, J.A.; Yusuff, A.A. A Fault Classification and Localization Method in A Power Distribution Network. In Proceeding of the IEEE Africon, Cape Town, South Africa, 18–20 September 2017.
3. Aucoin, B.M.; Jones, R.H. High Impedance Fault Implementation. *IEEE Trans. Power Deliv.* **1996**, *11*, 139–148.
4. Silva, S.; Costa, P.; Gouvea, M.; Lacerda, A.; Alves, F.; Leite, D. High impedance fault detection in power distribution systems using wavelet transform and evolving neural network. *Electr. Power Syst. Res.* **2018**, *154*, 474–483.
5. Nikander, A.; Jarventausta, P. Methods for earth fault identification and distance estimation in a compensated medium voltage distribution network. In Proceedings of the Energy Management and Power Delivery, Singapore, 3–5 March 1998.
6. AL-Dabbagh; Technisearch, M. High Impedance Fault Detector. Australian Patent PL3451, July 1992.
7. Jeerings, I.; Linders, I.R. A Practical Protective Relay for Down Conductor Faults. *IEEE Trans. Power Deliv.* **1991**, *6*, 565–574.
8. Reason, J. Relay Detects Down Wires by Fault Current Harmonics. *Electr. World* **1994**, *208*, 58–59.
9. Li, K.K.; Chan, W.L. Novel Methods for High-Impedance Ground Fault Protection in Low-Voltage Supply Systems. *Electr. Power Compon. Syst.* **2003**, *33*, 1133–1150.
10. Cui, Q.; El-Arroudi, K.; Weng, Y. A Feature Selection Method for High Impedance Fault Detection. *IEEE Trans. Power Deliv.* **2019**, *34*, 1203–1215.
11. Langeroudi, A.T.; Abdelaziz, M.M. Preventative high impedance fault detection using distribution system state estimation. *Electr. Power Syst. Res.* **2020**, *186*, 1–11.
12. Chen, J.C.; Phung, B.T.; Wu, H.W.; Zhang, D.M.; Blackburn, T. Detection of High Impedance Faults using wavelet transform. In Proceedings of the Australasian Universities Power Engineering Conference (AUPEC), Perth, Australia, 28 September–1 October 2014.
13. Lai, T.; Snider, L.; Lo, E.; Sutanto, D. High-Impedance Fault Detection Using Discrete Wavelet Transform and Frequency Range and RMS Conversion. *IEEE Trans. Power Deliv.* **2005**, *20*, 397–407.
14. Sedighi, A.-R.; Haghifam, M.-R.; Malik, O.; Ghassemian, M.-H. High Impedance Fault Detection Based on Wavelet Transform and Statistical Pattern Recognition. *IEEE Trans. Power Deliv.* **2005**, *20*, 2414–2421.
15. Baqui, I.; Zamora, I.; Mazón, J.; Buigues, G. High impedance fault detection methodology using wavelet transform and artificial neural networks. *Electr. Power Syst. Res.* **2011**, *81*, 1325–1333.
16. Huang, S.-J.; Hsieh, C.-T. High-impedance fault detection utilizing a Morlet wavelet transform approach. *IEEE Trans. Power Deliv.* **1999**, *14*, 1401–1410.
17. Elkalashy, N.I.; Lehtonen, M.; Darwish, H.A.; Taalab, A.-M.I.; Izzularab, M.A. DWT-based extraction of residual currents throughout unearthed MV networks for detecting high-impedance faults due to leaning trees. *Eur. Trans. Electr. Power* **2007**, *17*, 597–614.
18. Tyska, W.; Russell, B.D.; Aucoin, B.M. A Microprocessor-Based Digital Feeder Monitor with High Impedance Fault Detection. In Proceedings of the 47th Annual Texas A&M Relay Conference, College Station, TX, USA, 21–23 March 1994.
19. Butler, K.; Momoh, J. Neural network-based classification of arcing faults in a power distribution system. In Proceedings of the Protection of the North American Power symposium, Washington, DC, USA, 11–12 October 1993.
20. Snider, L.; Yuen, Y. The artificial neural-networks-based relay algorithm for the detection of stochastic high impedance faults. *Neurocomputing* **1998**, *23*, 243–254.
21. Lai, T.M.; Snider, L.A.; Lo, E.; Cheung, C.H.; Chan, K.W. High impedance faults detection using artificial neural network. In Proceedings of the Sixth International Conference on Advances in Power System Control, Operation and Management, Hong Kong, China, 11–14 November 2003.
22. Moloi, K.; Jordaan, J.A.; Hamam, Y. A hybrid method for high impedance fault classification and detection. In Proceedings of the Southern African Universities Power Engineering Conference/Robotics Mechatronics/Pattern Recognition Association of South Africa, Bloemfontein, South Africa, 28–30 January 2019.
23. Sheng, Y.; Rovnyak, S. Decision Tree-Based Methodology for High Impedance Fault Detection. *IEEE Trans. Power Deliv.* **2004**, *19*, 533–536.
24. Shahrtash, S.M.; Sarlak, M. High Impedance Fault Detection Using Harmonics Energy Decision Tree Algorithm. In Proceedings of the International Conference on Power System Technology, Chongqing, China, 28 September–1 October 2006.
25. Rai, K.; Hojatpanah, F.; Ajaei, F.B.; Grolinger, K. Deep Learning for High-Impedance Fault Detection: Convolutional Autoencoders. *Energies* **2021**, *14*, 3623.
26. Sulaiman, M.B.; Tawafan, A.H.; Ibrahim, Z.B. Detection of High Impedance Fault Using Probabilistic Neural Network Classifier. *J. Theor. Appl. Inf. Technol.* **2013**, *53*, 180–191.
27. Wang, S.; Dehghanian, P. On the Use of Artificial Intelligence for High Impedance Fault Detection and Electrical Safety. *IEEE Trans. Ind. Appl.* **2020**, *56*, 7208–7216.
28. Lala, H.; Karmakar, S. Detection and Experimental Validation of High Impedance Arc Fault in Distribution System Using Empirical Mode Decomposition. *IEEE Syst. J.* **2020**, *14*, 3494–3505.

29. Yang, M.T.; Gu, J.C.; Guan, J.L.; Cheng, C.Y. Detection of high impedance faults in distribution system. In Proceedings of the 2005 IEEE/PES Transmission & Distribution Conference & Exposition: Asia and Pacific, Dalian, China, 18 August 2005.
30. Wang, S.; Dehghanian, P.; Li, L.; Wang, B. A machine learning approach to detection of geomagnetically induced currents in power grids. *IEEE Trans. Ind. Appl.* **2019**, *56*, 1098–1106.
31. Wang, S.; Dehghanian, P.; Li, L. Power grid online surveillance through PMU-embedded convolutional neural networks. *IEEE Trans. Ind. Appl.* **2019**, *56*, 1146–1155.
32. Yusuff, A.A.; Fei, C.; Jimoh, A.; Munda, J.L. Fault location in a series compensated transmission line based on wavelet packet decomposition and support vector regression. *Electr. Power Syst. Res.* **2011**, *81*, 1258–1265.
33. Jadhav, A.; Thakur, K. Fault Detection and Classification in Transmission Lines Based on Wavelet Transform. *Int. J. Sci. Eng. Res.* **2015**, *3*, 14–19.
34. Keerthana, G.; Umayal, S.P. Analysis of faults in transmission line with the help of discrete wavelet transform. In Proceedings of the International Conference on Current Research in Engineering Science and Technology, Hyderabad, India, 5–27 October 2016.
35. Ray, P.K.; Mohanty, S.R.; Kishor, N.; Catalão, J.P.S. Optimal Feature and Decision Tree-Based Classification of Power Quality Disturbances in Distributed Generation System. *IEEE Trans. Sustain. Energy* **2014**, *5*, 200–208.
36. Moloi, K.; Jordaan, J.A.; Hamam, Y. High impedance fault detection technique based on Discrete Wavelet Transform and support vector machine in power distribution networks. In Proceedings of the IEEE Africon, Cape Town, South Africa, 18–20 September 2017.
37. HLivani, H.; Evrenosoglu, C.Y. A Fault Classification and Localization Method for Three-Terminal Circuits Using Machine Learning. *IEEE Trans. Power Deliv.* **2013**, *28*, 2282–2290.
38. Nakho, A.; Moloi, K.; Hamam, Y. Hig Impedance Fault Detection Based on HS-Transform and Decision Tree Techniques. In Proceedings of the IEEE Southern African Universities Power Engineering Conference/Robotics and Mechatronics/Pattern Recognition Association of South Africa, Potchefstroom, South Africa, 27–29 January 2021.
39. Sedighizadeh, M.; Rezazadeh, A.; Elkalashy, N.I. Approaches in High Impedance Fault Detection—A Chronological Review. *Adv. Electr. Comput. Eng.* **2010**, *10*, 114–128.